

^{186}Os – ^{187}Os systematics of Gorgona Island komatiites: implications for early growth of the inner core

Alan D. Brandon^{a,*}, Richard J. Walker^b, Igor S. Puchtel^c, Harry Becker^b,
Munir Humayun^c, Sidonie Revillon^d

^a NASA Johnson Space Center, Mail Code SR, Building 31, Room 114 Houston, TX 77058 USA

^b Isotope Geochemistry Laboratory, Department of Geology, University of Maryland at College Park, College Park, MD 20742, USA

^c Department of the Geophysical Sciences, The University of Chicago, 5734 S. Ellis Avenue, Chicago, IL 60637, USA

^d Southampton Oceanography Centre, School of Ocean and Earth Science, Waterfront Campus, European Way, Southampton SO14 3ZH, UK

Received 10 July 2002; received in revised form 15 October 2002; accepted 15 November 2002

Abstract

The presence of coupled enrichments in $^{186}\text{Os}/^{188}\text{Os}$ and $^{187}\text{Os}/^{188}\text{Os}$ in some mantle-derived materials reflects long-term elevation of Pt/Os and Re/Os relative to the primitive upper mantle. New Os data for the 89 Ma Gorgona Island, Colombia komatiites indicate that these lavas are also variably enriched in ^{186}Os and ^{187}Os , with $^{186}\text{Os}/^{188}\text{Os}$ ranging between 0.1198397 ± 22 and 0.1198470 ± 38 , and with γ_{Os} correspondingly ranging from +0.15 to +4.4. These data define a linear trend that converges with the previously reported linear trend generated from data for modern Hawaiian picritic lavas and a sample from the ca. 251 Ma Siberian plume, to a common component with a $^{186}\text{Os}/^{188}\text{Os}$ of approximately 0.119870 and γ_{Os} of +17.5. The convergence of these data to this Os isotopic composition may imply a single ubiquitous source in the Earth's interior that mixes with a variety of different mantle compositions distinguished by variations in γ_{Os} . The ^{187}Os - and ^{186}Os -enriched component may have been generated via early crystallization of the solid inner core and consequent increases in Pt/Os and Re/Os in the liquid outer core, with time leading to suprachondritic $^{186}\text{Os}/^{188}\text{Os}$ and γ_{Os} in the outer core. The presence of Os from the outer core in certain portions of the mantle would require a mechanism that could transfer Os from the outer core to the lower mantle, and thence to the surface. If this is the process that generated the isotopic enrichments in the mantle sources of these plume-derived systems, then the current understanding of solid metal–liquid metal partitioning of Pt, Re and Os requires that crystallization of the inner core began prior to 3.5 Ga. Thus, the Os isotopic data reported here provide a new source of data to better constrain the timing of inner core formation, complementing magnetic field paleointensity measurements as data sources that constrain models based on secular cooling of the Earth.

Published by Elsevier Science B.V.

Keywords: osmium; platinum; rhenium; komatiite

* Corresponding author. Tel.: +1-281-244-6408; Fax: +1-281-483-1573.

E-mail address: alan.d.brandon1@jsc.nasa.gov (A.D. Brandon).

1. Introduction

The Earth has undergone convective and conductive cooling since its formation ~ 4.6 billion years ago. Convection produces melting within the interior and material transport from the interior to the surface of the Earth. Convection also results in material exchange between the upper and lower mantle [1], and possibly between the core and the mantle [2,3]. Intimately coupled with the mechanisms of cooling and convection of the Earth's interior is the formation and crystallization of the iron-rich inner core, which is controlled by heat flux across the core–mantle boundary and the earliest thermal state of the Earth [4,5]. Therefore, constraining the onset of inner core crystallization and the rate of crystallization over time is important for examining the formation, cooling, and chemical evolution of the Earth, and for understanding the factors that controlled the generation of the geodynamo in the past [6].

Walker et al. [7] proposed that the coupled ^{187}Re – ^{187}Os and ^{190}Pt – ^{186}Os radiogenic isotope systems might serve as a tracer of inner core growth and core–mantle interaction. The capabilities of this potential tracer system are based on the assumption that inner core crystallization has resulted in predictable increases in Re/Os and Pt/Os ratios in the liquid outer core, relative to the presumably chondritic ratios in the bulk core. Consequently, the outer core would have evolved over time to more radiogenic $^{186}\text{Os}/^{188}\text{Os}$ and $^{187}\text{Os}/^{188}\text{Os}$ ratios than the generally chondritic convecting upper mantle. The rate of inner core crystallization and the relative and absolute partitioning behaviors of Pt, Re, and Os are the key parameters that govern the $^{186}\text{Os}/^{188}\text{Os}$ and $^{187}\text{Os}/^{188}\text{Os}$ ratios of the outer core.

Recent investigations have reported coupled variations in $^{186}\text{Os}/^{188}\text{Os}$ – $^{187}\text{Os}/^{188}\text{Os}$ ratios for picritic lavas from the modern Hawaiian plume and a picritic intrusion from the 251 Ma Siberian plume [8–10]. The relative enrichments in both isotope systems are comparable to those predicted by Walker et al. [7] for outer core–mantle interactions. If the coupled enrichments do reflect an addition of Os from the outer core to the plumes,

the data place minimum limits on the $^{186}\text{Os}/^{188}\text{Os}$ and $^{187}\text{Os}/^{188}\text{Os}$ ratios of the present-day outer core of ≥ 0.119849 and ≥ 0.140 , respectively [9]. In addition, Os-rich alloys from placer deposits thought to be derived from Phanerozoic peridotites in SW Oregon may also indicate the presence of early fractionation between Pt and Os in their source, which has been argued to be the outer core [11,12].

Although these studies have revealed important information regarding the sources of plumes, additional evidence will be required to demonstrate that at least some plume-derived Os originated in the outer core. Furthermore, if additional precise information on the present-day and ancient Os isotopic compositions of the outer core can be obtained, then important constraints can potentially be placed on the crystallization rate of the inner core. This might then lead to re-evaluations of the cooling history of the Earth.

In order to further evaluate the coupled enrichments of $^{186}\text{Os}/^{188}\text{Os}$ and $^{187}\text{Os}/^{188}\text{Os}$ in the context of core–mantle exchange, initiation and rates of crystallization of the core, and ancient crustal recycling, new high-precision Os isotopic data from Gorgona Island, Colombia, komatiites were obtained in this study. These komatiites were derived from a mid-Cretaceous plume that initiated volcanism over a large area in the Caribbean, Central America, and northern South America [13–17]. The rocks are the youngest known komatiitic lavas, and their existence indicates unusually high temperatures in the mantle. The komatiites have initial γ_{Os} values ranging from -0.5 to $+12.4$ [18], where γ_{Os} is the percent deviation from a chondritic reference reservoir at a specified time [19,20]. This range in γ_{Os} is similar to the range measured for the Hawaiian picrites that show the coupled enrichments in $^{186}\text{Os}/^{188}\text{Os}$ and $^{187}\text{Os}/^{188}\text{Os}$ [9,10]. Hence, these rocks are ideal candidates to further examine the origins of coupled enrichments of $^{186}\text{Os}/^{188}\text{Os}$ and $^{187}\text{Os}/^{188}\text{Os}$ in plume materials.

2. Samples

The detailed geologic setting, petrology, and

geochemistry of the komatiites from 20 km² Gorgona Island, which resides off the Pacific Coast of Colombia, is presented elsewhere [13,17–19,21]. Argon isotopic results for Gorgona komatiites and basalts indicate eruptive ages of 86–92 Ma with an average of 88 Ma [21,22]. A Re–Os isochron for basalts that are spatially associated with the komatiites also indicates crystallization approximately 89 Ma ago [18]. Despite the large range in initial Os isotopic compositions for the komatiites [18,19], initial ϵ_{Nd} values are relatively uniform at 10 ± 1 , indicating a homogeneous source with long-term depletion in Nd/Sm ratio [13,15,21,23].

Samples from two different Gorgona komatiite collections were selected for Os isotopic measurements in this study (Table 1). Samples 92-31, 94-7A,B, and 92-11 are from one of these suites [13], while sample 521 is from a second suite [17].

3. Analytical techniques

Rhenium, Pt, and Os concentration data were obtained on aliquots of each sample via isotope dilution in tandem with three different digestion/spike equilibration methods. This approach was taken in order to assess sample heterogeneity and sample–spike equilibration issues (see Section 4). In addition, because Pt concentrations cannot be obtained by thermal ionization mass spectrometry, it was necessary to measure replicates for concentrations using inductively coupled plasma mass spectrometry (ICP-MS).

Most samples were digested for Re, Pt and Os concentrations by the Carius tube method [24]. Three sample powders were analyzed for Re and Os concentration by sodium peroxide (alkaline) fusion [25]. One sample was analyzed for Re and Os concentration, using the NiS fire assay fusion [26]. For the Carius tube method, 2 g of sample powder was spiked and dissolved in inverse aqua regia at 230°C in a glass tube. Osmium was separated from the matrix via carbon tetrachloride solvent extraction [27] and purified by microdistillation [28]. Rhenium and platinum were separated and purified by ion exchange chro-

matography. Procedural blanks were 4 ± 2 pg for Re, 67 ± 5 pg for Pt, and 3 ± 1 pg for Os, resulting in blank corrections of approximately $\leq 0.1\%$, $\leq 0.5\%$, and $\leq 0.1\%$ on their concentrations, respectively. The procedural blanks had $^{187}\text{Os}/^{188}\text{Os}$ of 0.175 ± 0.005 .

The alkaline fusion technique was used as an alternative digestion technique [25]. Because of the relatively large amount (1 g) of komatiite sample analyzed, 6 g NaOH and 4 g of Na₂O₂ was used and the temperature was held at 600°C for 60 min. After digestion, the fusion cake was dissolved in H₂SO₄ to yield an approximately 6 N solution, then distilled in a conventional distillation apparatus using 15 ml of a 30% solution of H₂O₂ as oxidant and 3 ml 8.8 M HBr as the trap solution. The Os fraction was further purified by microdistillation. A total chemistry blank measured with this batch of samples was 50 pg for Re and 2 pg for Os, resulting in blank corrections of $\leq 5\%$ and $\leq 0.15\%$, respectively.

A 2 g aliquot of one sample (94-7 Powder B, Table 1) was spiked and processed using NiS fire assay at the University of Maryland [10,6,29]. The procedural blanks were 30 pg for Re, and 2 pg for Os, resulting in blank corrections of 2.9% and $< 0.15\%$, respectively.

For obtaining high-precision analyses of Os isotopes, 50–100 g of unspiked sample were fused using the NiS fire assay procedure [10,26]. For one sample (GOR 92-11), the Os concentration was 33 ppb (Table 1). Only 2 g of this sample was sufficient for the high-precision measurements, and hence, unspiked aliquots were processed via the Carius tube method for these analyses. Osmium was extracted and purified using the procedures listed above for the spiked samples. Two different Os blanks were 0.44 and 1.0 pg per g of fused sample, and have $^{186}\text{Os}/^{188}\text{Os} = 0.1199 \pm 0.0002$, and $^{187}\text{Os}/^{188}\text{Os} = 0.124 \pm 0.005$. Corrections to the sample ratios are included in the uncertainties cited (Table 1).

The Re and Os isotopic ratios for the concentration analyses were measured as oxides using a single-collector NBS-style mass spectrometer at the University of Maryland in the negative ion mode [10]. The Os and Pt isotopic ratios for the concentration analyses at the University of Chi-

Table 1
Re–Pt–Os isotopic systematics of the Gorgona komatiites

Sample		Re	Os	Pt	¹⁸⁷ Re/ ¹⁸⁸ Os	¹⁹⁰ Pt/ ¹⁸⁸ Os	¹⁸⁴ Os/ ¹⁸⁸ Os	¹⁸⁶ Os/ ¹⁸⁸ Os	¹⁸⁷ Os/ ¹⁸⁸ Os	γ _{Os}
GOR 92-31	CT ^b	0.9356	2.038		2.213(10)				0.12980(30)	+0.1
	CT ^c		2.38	11.08		0.004304				
	Na peroxide fusion ^a	1.056	2.463		2.067(20)				0.13056(15)	+0.85
							0.001309(9)	0.1198444(79)	0.1320275(110)	
							0.001338(8)	0.1198377(70)	0.1316211(80)	
GOR 94-7 Powder A							0.001309(10)	0.1198408(96)	0.1317552(203)	
							0.001329(12)	0.1198417(121)	0.1316061(141)	
	Average							0.1198411(28)	0.13175(19)	
	Age-corrected							0.1198405		
	CT ^a	0.9374	0.990		4.566				0.13585(13)	+2.1
Powder B	CT ^b	1.089	1.096		4.793				0.13516(22)	+1.3
	CT ^b	1.090	0.9732		5.404(8)				0.13637(6)	+1.5
	Na peroxide fusion ^a	1.305	1.674		3.759				0.13445(16)	+1.9
	CT ^a	0.520	0.925		2.710				0.13656(30)	+4.9
	CT ^c		1.144	15.27		0.012248				
GOR 92-11	NiS fusion ^a	0.9343	0.6865		6.560				0.14108(27)	+3.9
	Na peroxide fusion ^a	0.936	1.305		3.443				0.13669(19)	+4.1
							0.001316(6)	0.1198523(61)	0.1421662(78)	
							0.001312(7)	0.1198478(68)	0.1421652(72)	
							0.001327(7)	0.1198457(73)	0.1426703(102)	
	Average							0.1198486(38)	0.14233(34)	
	Age-corrected							0.1198470		
	CT ^b	0.6924	33.18		0.1005(18)				0.12628(30)	−0.2
	CT ^b	0.4336	31.29		0.0668(40)				0.12709(4)	+0.5
	CT ^c		36.97	8.487		0.000212				
GOR 521							0.001375(6)	0.1198410(69)	0.1270800(81)	
							0.001455(10)	0.1198415(110)	0.1270771(150)	
							0.001309(6)	0.1198366(67)	0.1270302(58)	
							0.001314(5)	0.1198396(74)	0.1270231(64)	
	Average							0.1198397(22)	0.127052(30)	
	Age-corrected							0.1198397		
	CT ^a	1.826	1.475		5.9834				0.13865(19)	+2.7
	CT ^c		1.712	16.602		0.0089				
							0.0013022(32)	0.1198458(32)	0.1380244(31)	
							0.0013001(27)	0.1198470(30)	0.1380233(31)	
Average							0.1198464(12)	0.138024(1)		
Age-corrected							0.1198452			

Re, Os and Pt concentrations are in parts per billion. Initial γ_{Os} is calculated for 89 Ma, relative to average chondrite (using equation 1 of [20]).

^a New data UMD.

^b [18].

^c New data UofC.

cago were measured using a ‘ThermoFinnigan Element’ high-resolution ICP-MS, equipped with a CETAC Technologies MCN6000 desolvating nebulizer [29,30]. Typical count rates were 10^5 – 10^6 cps for all elements, and internal precisions of individual runs were between ± 0.2 – 0.5% ($2\sigma_{\text{aver}}$). Long-term reproducibility of a 1 ppb Os- and 0.54 ppb in-house Pt-bearing standard solution, which characterizes the external precision of the analysis, was better than $\pm 1\%$ ($2\sigma_{\text{pop}}$) on all isotope ratios [30].

With the exception of sample GOR 521, the high-precision Os isotopic measurements were performed on a seven-Faraday cup mass spectrometer (VG Sector 54) in dynamic mode at the University of Maryland [10]. For sample GOR 521, high-precision measurements were performed in static mode on an eight-Faraday cup mass spectrometer (ThermoFinnigan Triton) at the Johnson Space Center. Signals of 80–150 mV on mass 234 ($^{186}\text{Os}^{16}\text{O}_3^-$) and 235 ($^{187}\text{Os}^{16}\text{O}_3^-$) were generated for 100 or more ratios to reach the desired internal run precision of ± 50 – 80 ppm (2σ) for $^{186}\text{Os}/^{188}\text{Os}$ and $^{187}\text{Os}/^{188}\text{Os}$. The interference of $^{186}\text{W}^{16}\text{O}_3^-$ on $^{186}\text{Os}^{16}\text{O}_3^-$ was monitored by measuring $^{184}\text{Os}^{16}\text{O}_3^-$ ($^{184}\text{W}^{16}\text{O}_3^-$, [10]). In one case, two replicate runs of one filament for GOR 92-11 have high $^{184}\text{Os}/^{188}\text{Os}$ ratios (Table 1). The $^{186}\text{Os}/^{188}\text{Os}$ values for these two runs are within error of those for the other runs for this sample. If $^{186}\text{W}^{16}\text{O}_3^-$ is present it should produce an interference that is 1.073 times larger than that for $^{184}\text{W}^{16}\text{O}_3^-$ [10]. The $^{186}\text{Os}/^{188}\text{Os}$ values would be approximately 0.119906 and 0.119992, for the two runs with elevated $^{184}\text{Os}/^{188}\text{Os}$, far above the measured values (Table 1). It is likely that this interference is $^{195}\text{Pt}^{37}\text{Cl}^-$. PtCl^- ions are not produced at mass 234. Hence, no detectable W interferences were present in any of the measurements for high-precision Os isotopes. The mean for 42 runs of the Johnson–Matthey Os standard at the University of Maryland was 0.1198471 ± 9 for $^{186}\text{Os}/^{188}\text{Os}$, and 0.1137989 ± 41 for $^{187}\text{Os}/^{188}\text{Os}$. The mean for five runs of the Johnson–Matthey Os standard during the analytical campaign at the Johnson Space Center was 0.1198466 ± 25 for $^{186}\text{Os}/^{188}\text{Os}$ and 0.1138068 ± 32 for $^{187}\text{Os}/^{188}\text{Os}$.

4. Results

Concentrations of Re and Os for the three komatiites analyzed were comparable to other Gorgona komatiites [18,19], with Re and Os concentrations ranging from 0.520 to 1.83 ppb and 0.925 to 2.46 ppb, respectively. Peridotite 92-11 contains unusually high concentrations of Os (> 30 ppb) and low Re (< 0.7 ppb). Platinum concentrations for all four samples range only from 11.1 to 16.6 ppb. Replicates of Re and Os concentrations using both Carius tube and Na peroxide fusion methods are within ± 6 – 28% (Table 1). Such ranges for concentrations are typical for these elements as a likely result of the nugget effect [20] and do not appear to result from incomplete sample–spike equilibration or variable access to these elements using these two different digestion techniques [20,24,25]. This is because, despite the measured Re and Os isotope heterogeneity of the different replicates, importantly, all of the corrected initial γ_{Os} values using all three techniques for each sample fall within these uncertainties. The initial γ_{Os} values for the four rocks, determined primarily by Carius tube digestion, range from -0.2 to $+4.9$. Uncertainties in the initial ratios corrected for ^{187}Re decay since crystallization are $< \pm 0.5$ γ_{Os} units [18], given the relatively low Re/Os ratios of the rocks and their relatively young age. The initial γ_{Os} values plotted in Fig. 1 are the average of the spiked replicates for each sample in Table 1 where high-precision $^{186}\text{Os}/^{188}\text{Os}$ was measured.

The $^{190}\text{Pt}/^{188}\text{Os}$ ratios for all four rocks range from 0.0002 to 0.0122. Given the long half-life of ^{190}Pt ($\lambda = 1.54 \times 10^{-12} \text{ a}^{-1}$) and $^{190}\text{Pt}/^{188}\text{Os}$ ratios that range only from 0.12 to 7 times the chondritic ratio (0.00174), the accumulation of ^{186}Os is not measurable over 89 Ma since formation. Hence, the measured and initial $^{186}\text{Os}/^{188}\text{Os}$ of all samples are identical within the cited analytical uncertainties. The $^{186}\text{Os}/^{188}\text{Os}$ ratios for these rocks range from 0.1198397 ± 22 (2σ of the mean) to 0.1198470 ± 38 . These data fall within the range of $^{186}\text{Os}/^{188}\text{Os}$ of 0.1198339 ± 28 to 0.1198475 ± 29 for Hawaiian picrites, and the data indicate that at least some portions of the mantle source of the Gorgona komatiites contain

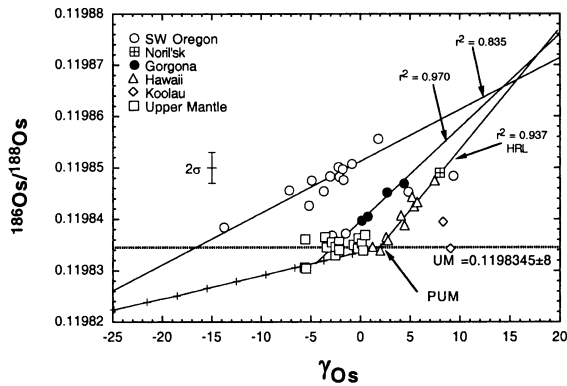


Fig. 1. A plot of $^{186}\text{Os}/^{188}\text{Os} - \gamma_{\text{Os}}$ for mantle materials and mantle-derived lavas. Regression lines for Hawaii [9,10] (HRL, Hawaii Regression Line), Gorgona (this study), and SW Oregon Os-rich alloy grains [11,12], are shown with calculated r^2 . The Primitive Upper Mantle (PUM) growth line is shown with plus symbols representing 500 Ma time intervals, where at time = 0: $^{186}\text{Os}/^{188}\text{Os} = 0.1198345$, $^{190}\text{Pt}/^{188}\text{Os} = 0.001734$, $\gamma_{\text{Os}} = 2.03$, $^{187}\text{Os}/^{188}\text{Os} = 0.1296$ [33], and $^{187}\text{Re}/^{188}\text{Os} = 0.4346$. The present-day upper mantle (UM) average composition for $^{186}\text{Os}/^{188}\text{Os}$ is shown that includes data for abyssal peridotites, and chromites and Os–Ir alloys from other ophiolites [8,9,31]. Four additional Os-rich alloy grain data from SW Oregon [12] are plotted that do not lie along the regression line. One data point, representing the Siberian plume, is plotted. Two Koolau picrites from Hawaii are shown [10]. The typical 2σ uncertainty for the mean of multiple analyses of each sample is shown. The initial γ_{Os} used for Gorgona data are the average of the replicates for each sample in Table 1 where high-precision $^{186}\text{Os}/^{188}\text{Os}$ was measured.

$^{186}\text{Os}/^{188}\text{Os}$ that is more radiogenic than the recent upper mantle.

The $^{187}\text{Os}/^{188}\text{Os}$ ratios of the samples determined by dissolving 2 g of sample using one of the three digestion techniques are in good agreement with the high-precision results determined by Ni–S fusion of 50–100 g of powder (Table 1). The one exception is sample GOR 94-7 (Table 1). Walker et al. [18] reported initial γ_{Os} values of +1.3 and +1.5 for duplicate analyses. Using powder made from the same hand specimen (Powder A), two additional aliquots analyzed for this study yield similar initial γ_{Os} values of +1.9 and +2.1. A second, larger batch of powder (Powder B), was processed from a second hand sample with the same sample name. Aliquots from this powder yield initial γ_{Os} using all three digestion

techniques averaging 4.4 ± 0.5 , which is significantly higher than the average value for Powder A ($+1.7 \pm 0.4$). Hence, we conclude that samples from two separate flows with different initial Os isotopic compositions were inadvertently given the same sample number. Only the hand sample from which Powder B was produced was sufficiently large to produce several hundred grams of sample, so although we report γ_{Os} values for both powders, high-precision $^{186}\text{Os}/^{188}\text{Os}$ measurements could only be made for Powder B.

5. Discussion

The four Gorgona samples form a linear array on a plot of $^{186}\text{Os}/^{188}\text{Os}$ versus γ_{Os} that is similar to, but not identical to the array generated for the combined Hawaiian and Siberian suites (Fig. 1). The Gorgona samples with the least radiogenic $^{186}\text{Os}/^{188}\text{Os}$ of 0.1198397 ± 22 and 0.1198405 ± 28 overlap within uncertainties of the range of ratios measured for upper mantle materials, including chromites and Os-rich alloys from ophiolite peridotites, and bulk abyssal peridotites [8–10,31]. Combined, these upper mantle materials define an average present-day $^{186}\text{Os}/^{188}\text{Os}$ of 0.1198345 ± 8 (2σ of the mean, $n = 18$). The most radiogenic Gorgona sample (GOR 94-7 Powder B) has $^{186}\text{Os}/^{188}\text{Os}$ of 0.1198470 ± 38 , that is within analytical uncertainties of the most radiogenic Hawaiian lava (Hualalai, 0.1198475 ± 29 [10]), but has a γ_{Os} value of +4.4 that is significantly less radiogenic than the Hawaiian lava (+7.5). Osmium-rich alloys from SW Oregon [11,12] that are thought to be derived from the Jurassic Josephine peridotite [32] have $^{186}\text{Os}/^{188}\text{Os}$ ratios that are more radiogenic than the defined present-day upper mantle and similar to both the Hawaiian picrite and Gorgona komatiite lavas. When compared, the data sets for Hawaii (and Siberia), Gorgona, and SW Oregon, define linear arrays in plots of $^{186}\text{Os}/^{188}\text{Os}$ versus γ_{Os} that converge to a common point (Fig. 1). Each of these linear arrays could reflect mixing between two distinct Os isotopic components where a common radiogenic isotopic component is present in the sources of all of these materials. This isotopic component

would have a present-day $^{186}\text{Os}/^{188}\text{Os}$ of about 0.119868–0.119872 and a γ_{Os} of +16 to +19 (Fig. 1). The possible origin of this component is evaluated below.

5.1. Crustal recycling

Crustal recycling has been frequently cited to explain ^{187}Os enrichments in ocean island basalt (OIB) sources [34,35], and also enrichments and depletions in other isotopic systems [36]. With regard to $^{187}\text{Os}/^{188}\text{Os}$ enrichments, this stems from the observation that recycled mafic crust contains two to three times the concentration of Re as fertile mantle, yet little Os. Consequently, the recycling of gabbroic or basaltic oceanic crust back into the mantle will lead to the generation of hybrid mantle with suprachondritic Re/Os, that over time will evolve to suprachondritic $^{187}\text{Os}/^{188}\text{Os}$ [19]. Because of the viability of crustal recycling models to explain many of the isotopic characteristics of OIBs, similar models involving crustal recycling have been proposed to account also for the coupled ^{186}Os – ^{187}Os systematics for the Hawaiian and Siberian systems [37]. The original models of mafic crustal recycling to explain enrichments in ^{187}Os in mantle sources [19,34,38], however, are problematic with regard to ^{186}Os enrichments, because mafic crust tends not to be appreciably enriched in Pt relative to fertile mantle. Consequently, recycling of mafic crust can, in some instances, account for enrichments in $^{187}\text{Os}/^{188}\text{Os}$, but cannot easily account for accompanying enrichments in $^{186}\text{Os}/^{188}\text{Os}$. For example, Brandon et al. [9,10] concluded that ancient crustal recycling could not explain the Hawaiian–Siberian Os data, based on two lines of evidence. First, simple mixing relationships show that large proportions (70% or more) of ancient recycled crust must be added to a peridotitic source to raise the $^{186}\text{Os}/^{188}\text{Os}$ of average upper mantle to the radiogenic ratios observed. High MgO magmas, such as the parental magmas of the Hawaiian picrites, cannot be produced from a hybrid source containing such large amounts of crust [39]. Second, no known crustal materials thought to be present in oceanic crust have the Pt/Re ratios (88–100) necessary to produce the observed

correlated coupled enrichments of $^{186}\text{Os}/^{188}\text{Os}$ and $^{187}\text{Os}/^{188}\text{Os}$. Instead, most crustal materials have Pt/Re ratios of ≤ 25 , consistent with the geochemical behavior of Pt and Re in crustal systems [10]. Thus, mixing ancient crustal materials with upper mantle will result in mixing lines with much shallower slopes in plots of $^{186}\text{Os}/^{188}\text{Os}$ versus $^{187}\text{Os}/^{188}\text{Os}$ than the linear correlation observed in the Hawaiian–Siberian data. Recently, however, it has been noted that some metalliferous sediments that formed via hydrothermal processes at the ocean–crust interface have Pt/Re ratios that are up to 645 [37,40]. In addition, some Fe–Mn-rich nodules also can have high Pt/Os and relatively low Re/Os [41]. The high Pt/Re characteristics of metalliferous sediments led Ravizza et al. [37] to suggest that, ‘while the existence of these high Pt/Re ratios in basal metalliferous sediments does not preclude a core–mantle boundary origin for the Hawaiian mantle plume, it does present a potentially viable alternative interpretation’. The viability of this hypothesis is further tested here considering the Hawaiian suite and the new Gorgona suite.

Mixing lines were calculated for mixtures of metalliferous sediment and fertile mantle (Fig. 2). For the calculations, Os isotopic compositions of the sediments (umbers) were modified to be consistent with 2 Ga of radiogenic ingrowth. Sample MF164F from the Ravizza et al. [37] suite with the highest Pt/Os (127.4) and Pt concentration (22.3 ppb), and having an initial $^{187}\text{Os}/^{188}\text{Os}$ of 0.505, was mixed with peridotite containing 3.1 ppb Os, a γ_{Os} of –3, and $^{186}\text{Os}/^{188}\text{Os}$ of 0.1198345 (mixing line 1, Fig. 2). This mixing line does not match the trends for either the Gorgona or Hawaiian data. The slope for the Gorgona trend can be artificially matched by either lowering the assumed initial $^{187}\text{Os}/^{188}\text{Os}$ of the 2 Ga aged umber to 0.3 (mixing line 2) or lowering the $^{187}\text{Re}/^{188}\text{Os}$ of the umber by a requisite amount. Either scenario requires open-system behavior of Re–Os since the formation of an umber that at 2 Ga was similar to MF164F. Sample MF164F is the only one reported by Ravizza et al. [37] for which mixing lines can potentially match the observed trends delineated by the Hawaiian or Gorgona suites. Other umbers that are aged 2 Ga produce

mixing lines that are much shallower than the one calculated using MF164F (e.g. mixing line 3). Thus, the presence of ancient recycled sediments in the mantle sources of some plume components might satisfactorily explain the Os isotopic systematics of only those plume-derived lavas that lie to the right of the linear trends defined by the Hawaiian and Gorgona data sets. Such rocks do exist, such as the Hawaiian Koolau picrites [10] that lie well below the trend for the other Hawaiian lavas (Fig. 2), and possibly the Os-rich alloy grains that plot to the right of the main trend of the SW Oregon data in Fig. 1 [11,12]. Indeed, the presence of recycled sediments in the source of the Koolau picrites is also consistent with O and Pb isotopic compositions [10,42].

It is possible that a metalliferous sediment may one day be discovered with Pt/Os and Re/Os ra-

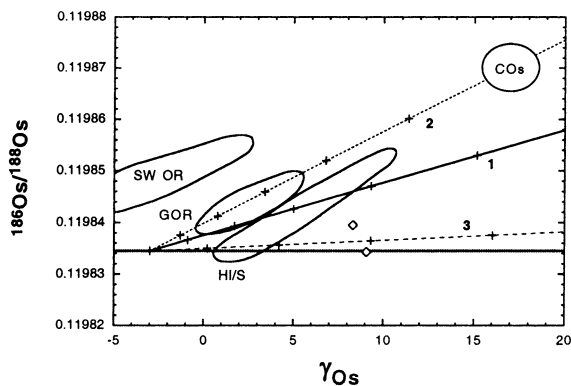


Fig. 2. Mixing lines between a peridotite (3.1 ppb Os, $^{186}\text{Os}/^{188}\text{Os} = 0.1198345$, $\gamma_{\text{Os}} = -3$) and metalliferous sediments [37] that have aged for 2 Ga. Fields for the SW Oregon Os-rich alloy (SW OR), Gorgona (GOR), and Hawaii–Siberia (HI/S), and the two data points for Koolau picrites (open diamonds), are shown. The area where the regression lines for the three data suites converge in Fig. 1 is shown as COs. Mixing line 1: for metalliferous sample MF164F aged for 2 Ga (Os = 0.175 ppb, $^{186}\text{Os}/^{188}\text{Os} = 0.1202$, $^{187}\text{Os}/^{188}\text{Os} = 0.5794$ ($\gamma_{\text{Os}} = 356.2$) and peridotite end-members defined in the text. Mixing line 2: the initial $^{187}\text{Os}/^{188}\text{Os}$ or $^{187}\text{Re}/^{188}\text{Os}$ of MF164F aged for 2 Ga is adjusted so that the mixing line will conform to the Gorgona data and pass through the COs composition, see text for explanation. Mixing line 3: for metalliferous sample MF 10S aged for 2 Ga (Os = 0.085 ppb, $^{186}\text{Os}/^{188}\text{Os} = 0.12004$, $^{187}\text{Os}/^{188}\text{Os} = 1.749$) mixed with peridotite. Increments of 10% mixing between the two components are shown (+).

tios that are sufficient to generate, over time, a reservoir with an Os isotopic composition that can be mixed with a mantle component to generate mixing lines on plots of $^{186}\text{Os}/^{188}\text{Os}$ versus $^{187}\text{Os}/^{188}\text{Os}$ that match those of the Hawaiian or Gorgona trends. However, several additional lines of evidence suggest that recycling of such sediment can never be considered a viable explanation for the Gorgona and Hawaiian data sets.

First, in the scenario where the sediment with the highest Pt concentration is used (22.3 ppb, MF164F), ~ 40 wt% of the umber is required in the mix in order to generate the samples from Gorgona with a $^{186}\text{Os}/^{188}\text{Os}$ of 0.119846 (Fig. 2). Allowing 3 Ga of radiogenic ingrowth, the proportion of umber necessary to produce a $^{186}\text{Os}/^{188}\text{Os}$ of 0.119846 matching mixing line 2 is $\sim 30\%$. The average Pt concentration of the umber data reported by Ravizza et al. [37] is 13.7 ppb. Using this Pt concentration with the other characteristics listed above, and allowing 3 Ga of radiogenic ingrowth, mixing line 2 will produce a $^{186}\text{Os}/^{188}\text{Os}$ of 0.119846 when $\sim 33\%$ of the hypothetical umber is added to a peridotitic source. Adding this amount of umber to a peridotite source will have identifiable petrological consequences. The umbers average 9 ± 3 MnO₂ and $53 \pm 13\%$ Fe₂O₃ [37]. Adding umber to the source of Hawaiian or Gorgona lavas will result in a hybrid source with anomalously high Mn and Fe and anomalously low Fe/Mn. For example, mixing an umber that has had 2 Ga of radiogenic Os ingrowth with peridotite will result in a mixing curve with large shifts in Mn content with little effect on the $^{186}\text{Os}/^{188}\text{Os}$ of the hybrid source, until at least 20% of the mixture is umber (Fig. 3). Partial melting of such a source with strongly elevated Mn contents would result in an easily detectable difference between the lavas that carry the coupled radiogenic Os signature (e.g. GOR 521, 94-7B, Loihi, Hualalai) relative to lavas derived from a mantle source that does not (e.g. GOR 92-31, Mauna Kea, Kilauea). But such lavas do not have highly variable Mn contents, nor are they elevated in Mn content (Fig. 3, [11,17,39]).

Second, metalliferous sediments are probably not of sufficient volume to generate significant

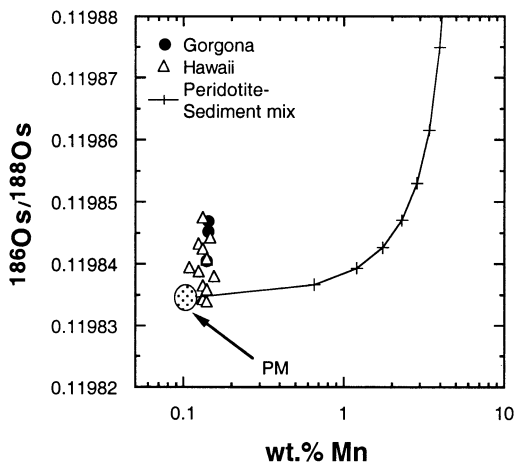


Fig. 3. A mixing model between peridotite (PM, where Mn is for pyrolite [43]) and average umbrae. The umbrae has 2 Ga of ^{186}Os ingrowth using the Pt/Os systematics of sample MF164F (same as for Mixing line 1 in Fig. 2), and Mn = 5.62 weight% (average of 19 umbrae [37]).

compositional heterogeneities in a large mantle plume, such as the Hawaiian or Caribbean plumes. The formation of metalliferous sediments, such as ochres and umbrae, occurs as a result of minor redistributions of Pt, Re and Os at the sea-water–oceanic floor interface. No new atoms of these elements are produced within this interface. As such, a volume of oceanic crust on the scale of 1 km^3 or larger that hosts metalliferous sediments will contain the same number of atoms of Pt, Re and Os as a similar volume of crust that lacks the sediments. Thus, recycling of high Pt/Os sediments can only affect the $^{186}\text{Os}/^{188}\text{Os}$ of a very small portion of the mantle. Third, these umbrae apparently require the oxidizing conditions found in modern marine sediments for the genesis of their high Pt/Re ratios. It is not known if conditions in the Archean and early Proterozoic were conducive to the formation of such sediments.

Finally, the fact that several independent data sets converge to a single area in $^{186}\text{Os}/^{188}\text{Os}$ versus γ_{Os} (Figs. 1 and 2), requires a component common to all of the suites. These data require that the same metalliferous sediments with the same Pt–Re–Os isotopic systematics reside in the mantle in widely dispersed locales. Hence, this umbrae recycling model requires special circumstances

that are not realistic. In conclusion, these considerations indicate that recycling of mafic oceanic crust, with or without accompanying sediments, is not consistent with the linear trends observed between $^{187}\text{Os}/^{188}\text{Os}$ and $^{186}\text{Os}/^{188}\text{Os}$. Ancient recycling is also inconsistent with the compositions of the MgO-rich lavas that are the basis for the linear trends that have been detected.

5.2. Convergence – outer core?

Plausible scenarios for the origin of the radiogenic Os isotopic component that lies at the juncture between the Hawaiian–Siberian and Gorgona data sets require that such a component is homogeneous and sufficiently pervasive to manifest itself in widely dispersed regions in the Earth’s mantle. That reservoir could be the outer core. Walker et al. [7] speculated that the entrainment of very small amounts of evolved outer core ($\leq 1\%$) into mantle at the core–mantle boundary could ultimately lead to the formation of an isotopically heterogeneous plume with respect to $^{187}\text{Os}/^{188}\text{Os}$ and $^{186}\text{Os}/^{188}\text{Os}$. This, they argued, could lead to the generation of plume-derived magmas with Os isotopic characteristics consistent with liquid metal–solid metal partitioning of Re, Pt and Os. Puchtel and Humayun [29] subsequently argued that Os and other highly siderophile elements might also be isotopically exchanged between the core and mantle, obviating the requirement for significant mass transfer of Fe and Ni from the core into the mantle. Indeed, as noted above, it has been concluded that the coupled enrichments of Os isotopes observed in the Hawaiian–Siberian data set are best explained via liquid metal–solid metal partitioning [8–10], as deduced from the relative fractionations between Pt, Re, and Os observed for asteroidal cores and for iron metal crystallization experimental partitioning data [44,45]. Meibom and Frei [12] also favored an outer core origin for the Os-rich alloy grains from SW Oregon that lie on the positive-sloped trend in Fig. 1. They too noted the possible importance of the zone of convergence between the linear trend of their data and the trend for the Hawaiian lavas (Fig. 1).

The addition of the Gorgona suite provides

more compelling evidence that the convergence zone is real, and does indeed require a significant reservoir from which mantle materials can periodically extract Os that is enriched in $^{187}\text{Os}/^{188}\text{Os}$ and $^{186}\text{Os}/^{188}\text{Os}$ relative to the contemporary convecting upper mantle. If this reservoir is the outer core, it places important constraints on the rate of inner core crystallization, and possibly the composition of the core. If the coupled enrichments in these suites reflect the presence of an outer core component, the convergence of the linear trends to a $^{186}\text{Os}/^{188}\text{Os}$ ratio of 0.119868–0.119872 and a γ_{Os} of +16 to +19 may reflect the Os isotopic composition of the evolved outer core within the last several hundred million years. This interpretation requires that the linear correlations defined by the Gorgona and Hawaiian data are mixing lines between relatively recent outer core and mantle components that range from depleted to undepleted, relative to the estimated composition of the primitive upper mantle (PUM, $\gamma_{\text{Os}} = +2$ at $T=0$ [33]). In the case of the Hawaiian suite, the end-member has a γ_{Os} value of approximately +1 to +2, consistent with some estimates of the composition of the modern convecting upper mantle and PUM [33,46]. For the Gorgona suite, the depleted mantle component had an initial γ_{Os} of approximately -3 , assuming this mantle component had a $^{186}\text{Os}/^{188}\text{Os}$ similar to the average upper mantle of 0.1198345 at the time of eruption, or -5 extrapolating back to a common PUM evolution trajectory of ^{186}Os – ^{187}Os (Fig. 1). None of the Gorgona komatiites have initial γ_{Os} values of < -0.5 [18], so there is no direct Os isotopic evidence for a depleted source. However, the initial ϵ_{Nd} values for Gorgona komatiites ranging from +9.2 to +11.4 indicate a source that experienced long-term depletion in the Nd/Sm ratio ([17,18] and references therein). The extrapolated end-member γ_{Os} value of -3 to -5 may be within the range of variation in the convecting upper mantle [31,47]. Alternatively, it may represent derivation from a reservoir other than the convecting upper mantle, that is somewhat more depleted than the convecting upper mantle, such as recycled ancient, melt-depleted lithospheric mantle [33]. The data array linear trend defined by most of the Os-rich alloy grains

analyzed from SW Oregon is more problematic, given the interpretation of an outer core origin and mixing. Unlike for the Gorgona and Hawaiian trends, the trend for these grains extrapolates to a point that is consistent with approximately chondritic initial ratios for both $^{186}\text{Os}/^{188}\text{Os}$ and $^{187}\text{Os}/^{188}\text{Os}$ during the first 500 Ma of Earth history (Fig. 1). Thus, if direct mixing with a source that lies along the chondritic evolution trajectory was involved, the depleted end-member is more depleted than any reservoir known to exist today. Instead of mixing, Meibom and Frei [12] implied that the grains formed directly from the Os metal that resided in the outer core. If the grains represent primary crystallization products of a major reservoir, then they essentially record the Os isotopic composition of that reservoir at the time they formed, given their extremely low Re/Os and Pt/Os ratios. Hence, the implication is that the least radiogenic of the samples formed at approximately 2.6 Ga [12].

In summary, additional documentation and considerations will be required to unravel the origins of the Os-rich alloy grains from SW Oregon. However, the combined relationships for Hawaii–Siberia, Gorgona, and, although viewed with caution, possibly the SW Oregon Os-rich alloy grains, indicate that a reservoir with distinct Os isotopic characteristics is present in the Earth that is prevalent enough to be manifested in mantle-derived materials in widely dispersed locations. This Os isotopic composition is consistent with the outer core model previously proposed [7–10] and will be further considered below.

5.3. Core crystallization

The convergence of the Os isotopic data in the Gorgona, Hawaiian–Siberian, and possibly the SW Oregon data sets may constrain the recent Os isotopic composition of the outer core, as supported by arguments presented above. From these data, the isotopic composition is estimated to be more radiogenic than the minimum estimate obtained from the Hawaiian data alone [9,10]. In this section, four different crystallization models for the Earth's core are evaluated in the context of the Os isotopic data presented above and those

from the literature, assuming that the point of convergence provides the Os isotopic composition of the modern outer core. The goal of this modeling is to draw comparisons with thermodynamic and geophysical models for the Earth's thermal cooling history, in order to determine which Os isotope outer core evolution scenarios are most realistic, and vice versa.

For the first three models, it is assumed that inner core crystallization began at 4.4 Ga (Fig. 4). Inner core crystallization proceeds to 5.5%, which is the present-day weight percent of the bulk core [7]. In Model 1, the core undergoes very rapid crystallization in the first 100 Ma of inner core growth, such that most of the inner core is crystallized by 4.3 Ga (based on [7,12]). In Model 2, the core undergoes rapid crystallization during the Archean, followed by slower, but constant crystallization in post-Archean times (hybrid between Models 1, 3 and 4). In Model 3, the inner core is crystallized at a constant crystallization rate over Earth history (based on [5]). Finally, in Model 4, core crystallization is delayed until 3.5 Ga, wherein the core undergoes rapid crystallization during the Archean followed by slower, but constant rate of crystallization during the post-Archean (based on [4]).

Parameters used and resultant Os isotopic evolution growth curves are presented in Table 2 and Figs. 4–6. For these models, the solid metal–liquid

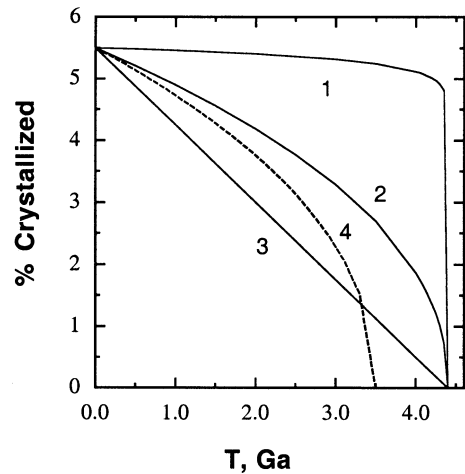


Fig. 4. Diagram illustrating the percent of core crystallized to 5.5% over time for Models 1–4 in Table 2.

metal partition coefficients ($D_{\text{sm/lm}}$) for Re and Os necessary for producing a present-day $^{186}\text{Os}/^{188}\text{Os} = 0.119870$ and $\gamma_{\text{Os}} = +17.5$ (i.e. the approximate convergence point of the Gorgona and Hawaii data) were adjusted assuming D_{Pt} was 2.9 [7]. In order to determine which D s may be acceptable for simulating Re and Os behavior in the Earth's core, the calculated D s for the four models are compared to the range in D s obtained for high-pressure experiments [44] in Fig. 5. The D s required for the four models mostly plot within un-

Table 2
Parameters for core crystallization models of Fig. 4

	Model 1, Rapid ^a	Model 2, Intermediate ^a	Model 3, Constant ^a	Model 4, Intermediate delay start ^b
D_{Pt}	2.9	2.9	2.9	2.9
D_{Re}	18.25	22.7	26.2	24.1
D_{Os}	28.2	36.4	44.2	40.4
@ 5.5% crystallization and 0 Ma:				
Pt (ppm)	5.254	5.254	5.254	5.254
Re (ppm)	0.096	0.075	0.061	0.069
Os (ppm)	0.661	0.415	0.267	0.332
$^{186}\text{Os}/^{188}\text{Os}$	0.119870	0.119870	0.119870	0.119870
$^{190}\text{Pt}/^{188}\text{Os}$	0.00736	0.01199	0.0180	0.0145
γ_{Os}	+17.5	+17.5	+17.5	+17.5
$^{187}\text{Re}/^{188}\text{Os}$	0.7055	0.8723	1.1125	1.0105

^a Starting parameters at 4.4 Ga: Pt = 5.85 ppm, Os = 3.08 ppm, Re = 0.2552 ppm, $^{186}\text{Os}/^{188}\text{Os} = 0.11982266$, $^{190}\text{Pt}/^{188}\text{Os} = 0.00174$, $\gamma_{\text{Os}} = 0$, $^{187}\text{Re}/^{188}\text{Os} = 0.4018$.

^b Starting parameters at 3.5 Ga: Pt = 5.85 ppm, Os = 3.08 ppm, Re = 0.2552 ppm, $^{186}\text{Os}/^{188}\text{Os} = 0.11982509$, $^{190}\text{Pt}/^{188}\text{Os} = 0.00174$, $\gamma_{\text{Os}} = 0$, $^{187}\text{Re}/^{188}\text{Os} = 0.4018$.

certainty of those obtained for the experiments, with two exceptions. The D_{Os} for the constant growth Model 3 is $\sim 39\%$ higher (44.2 versus 31.7 ± 2.36) and for delayed growth Model 4 is $\sim 27\%$ higher (40.4) than the range observed in the experiments (Fig. 5). However, given the unknowns associated with simulating metal crystallization at the high temperatures and pressures of the Earth's core, the overall fit between the D_s calculated, based on Re–Pt–Os isotopic systematics in this study, and the D_s obtained in the experiments is strong support for the validity of the models presented here. In addition, the D_{Pt} of 2.9 is based on crystallization within the Group IIAB iron meteorite system [7,48]. For the experiments, D_{Pt} ranged from 0.6 to 3.9 [44]. If D_{Pt} is lowered in the crystallization models, there will be a corresponding reduction in both D_{Re} and D_{Os} . Also of note, the lower D_{Pt} and the higher D_{Re} and D_{Os} were obtained for experiments with larger amounts of light alloying components such as S and P [44]. The silicate–silicate melt D_s estimated for mantle melting ($D_{sil/silm}$) are also plotted in Fig. 5. These D_s do not match those for partitioning in Fe metal systems. The D_{Re} is several orders of magnitude lower, resulting in $D_{Os/Re}$ and $D_{Pt/Re}$ that are higher. Hence, processes that in-

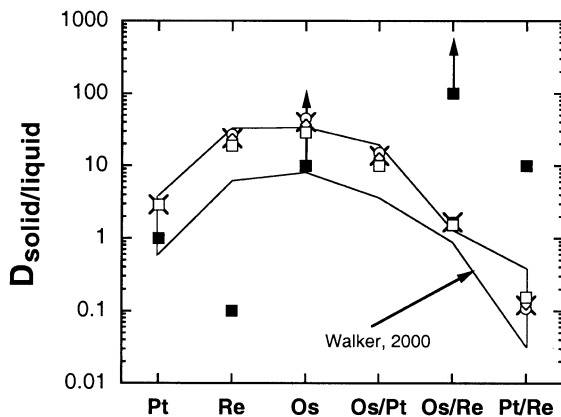


Fig. 5. The $D_{solid/liquid}$ for Pt, Re, Os and their ratios for metal crystallization or silicate mantle melting (solid squares). Symbols for models from Table 2 are: Model 1 (open squares), Model 2 (open diamonds), Model 3 (open circles), and Model 4 (crosses). The field for D_s obtained from high-pressure metal crystallization experiments [44] is also shown.

volve fractionation of these elements in Fe metal-free, silicate-rich systems cannot create the coupled ^{186}Os and ^{187}Os enrichments over Earth history.

The ramifications for explaining Os isotopic compositions of various sample suites with these core evolution models are presented in Fig. 6A,B, where the outer core evolution curves are plotted versus time. Several conclusions can be made regarding the crystallization history of the core. First, an end-member Os isotopic composition for any of the four outer core evolution models over time can explain the ^{187}Os -enriched lavas measured to date with the exception of modern to recent OIB with $\gamma_{Os} = \geq +17.5$ (Fig. 6B). This is because all of the lava data plot below the four model core evolution lines, and mixing between mantle components and outer core at any time in Earth history should produce a hybrid source that falls between these two end-members. Some OIB are more enriched in ^{187}Os than the present-day γ_{Os} of the outer core predicted by the convergence of Gorgona, Hawaii–Siberia, and the SW Oregon data (Fig. 2). These require an additional source of radiogenic ^{187}Os , likely ancient recycled crust [19,42]. However, as shown above and previously [9,10], ancient recycled crustal material cannot explain the coupled enrichments of both ^{186}Os and ^{187}Os in plume materials.

Second, if the constant crystallization (Model 3) or a delayed crystallization (Model 4) holds, then the lavas have completely inherited the outer core Os isotopic composition [29]. In contrast, the rapid and intermediate models (1 and 2) would result in an Os isotopic composition of the hybrid mantle source that is intermediate between the outer core and the original mantle composition (Fig. 6). Therefore, if material exchange between the outer core and the mantle results in complete transfer of the Os isotopic composition of the outer core across the core–mantle boundary, then rapid cooling of the Earth that resulted in early rapid inner core formation to near its present size is not required. Instead, core crystallization rates would be more consistent with a model where cooling of the Earth's deep interior was relatively slow. Third, data for the 2.8 Ga Kostomuksha komatiites and 2.7 Ga Belingwe komatiites indicate that

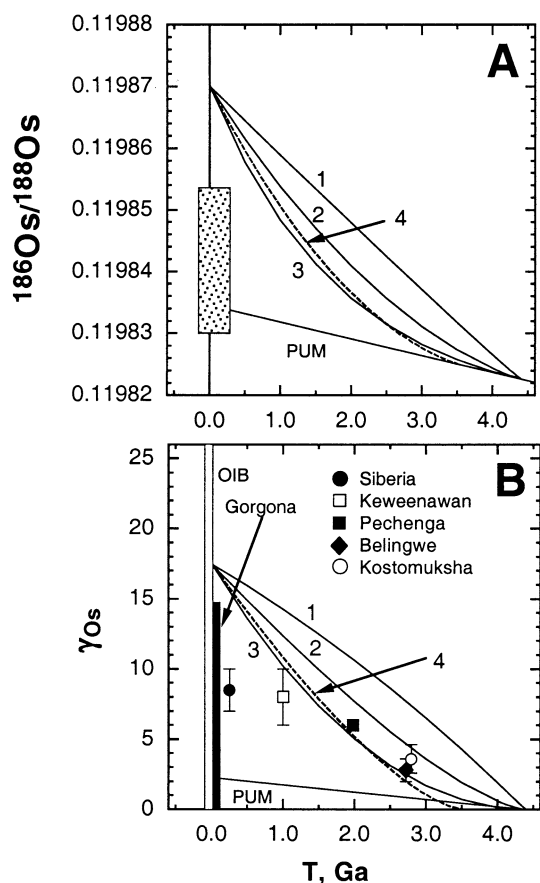


Fig. 6. Variations of $^{186}\text{Os}/^{188}\text{Os}$ and γ_{Os} over time for core evolution models 1–4 from Fig. 4 and Table 2. The PUM evolution lines are plotted. (A) The range in $^{186}\text{Os}/^{188}\text{Os}$ data for Gorgona (this study), Hawaii [9,10] and Siberian [8], data are plotted as a stippled box. (B) The range in γ_{Os} of modern OIB ([34,35,42,49] and references therein), Gorgona [18], Siberia [50,51], Keweenawan [52], Pechenga ferropicrites [53], Belingwe komatiites [54], and Kostomuksha komatiites [55] are shown.

mantle sources with γ_{Os} of approximately +3.0 existed by the late Archean [54,55]. These enrichments could be the result of either very early recycling of appreciable mafic crust into the sources of the komatiites, or an outer core origin for the Os. If the enrichments in these lavas over time reflect the evolving isotopic composition of Os in the outer core, then the inner core must have begun to crystallize at or prior to 3.5 Ga. Delaying the onset of inner core crystallization until 3.5

Ga or later would have difficulty explaining the Belingwe and Kostomuksha data at 2.7–2.8 Ga, unless D_{Os} and D_{Re} are much greater than those used in the models here and in the experiments [44]. Thus, the onset of inner core crystallization early in Earth history is considered to be consistent with these Os isotopic constraints, contrary to some secular cooling models [56–58], but consistent with others [4,5]. The average age of the inner core in Models 3 and 4 (i.e. the time at which half of the inner core is crystallized), are 2.25 and 2.75 Ga, respectively (Fig. 4). These average ages fall within the range of those calculated for the inner core integrated over Earth history on the basis of the heat loss models [59]. The age of the inner core could be as high as 2.7 Ga or as low as 1 Ga, depending on model assumptions and uncertainties, and the concentrations of U, Th, and K [59]. The concentrations of these elements are not precisely constrained at present and will depend on the bulk composition of the core, including what the light alloying component(s) is/are [60]. Therefore, within the present uncertainties in constraining the average age of the inner core, Models 3 and 4 presented here on the basis of Os isotopes are consistent with estimates obtained using geophysical and thermodynamic parameters [4,5,59].

6. Conclusions

The 89 Ma Gorgona komatiites have coupled enrichments of $^{186}\text{Os}/^{188}\text{Os}$ and $^{187}\text{Os}/^{188}\text{Os}$ similar to those displayed by the Hawaiian and Siberian plumes but with a different slope. It has been proposed that these coupled enrichments could be explained by adding ancient hydrothermally altered or metalliferous sediments into the source of these plumes [37]. Mixing models, however, convincingly show that sediment recycling cannot explain the correlated ^{186}Os – ^{187}Os systematics of the Hawaiian, Siberian or Gorgona suites. Adding these sediments to their plume sources would also result in strongly elevated Mn and Fe contents that are not observed. A model involving Os exchange during core–mantle interaction is able to explain the coupled Os isotopic variations of the

Gorgona, Hawaiian and Siberian plume data sets. This model has the advantage of reconciling why a common isotopic component exists in mantle-derived materials from widely dispersed locales, and points to a source that is relatively extensive and homogeneous in the Earth's interior.

If the coupled enrichments of $^{186}\text{Os}/^{188}\text{Os}$ and $^{187}\text{Os}/^{188}\text{Os}$ for these materials reflect the presence of outer core Os in the plumes, then the onset of core crystallization must have been within the first billion years of Earth history. Inner core crystallization must have begun relatively early in Earth history [4,5]. Models for the cooling history of the Earth that result in inner core crystallization commencing as late as 2–3 Ga [56–58] would be inconsistent with the putative evolution of Os isotopes in the outer core, given the solid metal–liquid metal partition coefficients used for generating the models. The average age of the inner core calculated from Os isotope evolution Models 3 and 4 presented here, that allows for constant inner core growth or onset of crystallization delayed until 3.5 Ga, respectively, fall within the range of integrated ages for the inner core over Earth history based on thermodynamic and geophysical parameterizations [59]. These comparisons are consistent with thermal cooling models where crystallization occurs progressively over 4.5 Ga, rather than rapid early crystallization followed by little crystallization of the inner core since the Archean.

High-precision ^{186}Os – ^{187}Os data for Proterozoic and Archean high-MgO lavas may ultimately provide clues towards further constraining the rate of inner core crystallization. Future work should be directed at performing high-precision $^{186}\text{Os}/^{188}\text{Os}$ measurements on ancient lavas where both chondritic and positive initial γ_{Os} have been demonstrated. Additional considerations of the mechanism of core–mantle exchange, and further partitioning experiments for highly siderophile elements are needed in conjunction with these measurements for better constraints on inner core crystallization and thermal cooling of the Earth over time. Such combined efforts will aid in further understanding the effects of core–mantle exchange on the highly siderophile budget of the silicate Earth.

Acknowledgements

This work was supported by NSF grants EAR 9910485 to A.D.B., EAR-CSEDI 0001921 to R.J.W., and EAR 0106974 to M.H. Journal reviews by Robert Frei, Chris Hawkesworth, Simon Turner, and one anonymous reviewer are gratefully acknowledged. [BW]

References

- [1] R.D. Van der Hilst, S. Widiyantoro, E.R. Engdahl, Evidence for deep mantle circulation from global tomography, *Nature* 386 (1997) 578–584.
- [2] L.H. Kellogg, S.D. King, Effect of mantle plumes on the growth of D' by reaction between the core and the mantle, *Geophys. Res. Lett.* 20 (1993) 379–382.
- [3] B.A. Buffett, E.J. Garnero, R. Jeanloz, Sediments at the top of the Earth's core, *Science* 290 (2000) 1338–1341.
- [4] D.J. Stevenson, T. Spohn, G. Schubert, Magnetism and thermal evolution of the terrestrial planets, *Icarus* 54 (1983) 466–489.
- [5] F.D. Stacey, D.E. Loper, Thermal histories of the core and mantle, *Phys. Earth Planet. Inter.* 36 (1984) 99–115.
- [6] B.A. Buffett, Earth's core and the geodynamo, *Science* 288 (2000) 2007–2012.
- [7] R.J. Walker, J.W. Morgan, M.F. Horan, ^{187}Os enrichment in some mantle plume sources: Evidence for core-mantle interaction?, *Science* 269 (1995) 819–822.
- [8] R.J. Walker, J.W. Morgan, E. Beary, M.I. Smoliar, G.K. Czamanske, M.F. Horan, Applications of the ^{190}Pt – ^{186}Os isotope system to geochemistry and cosmochemistry, *Geochim. Cosmochim. Acta* 61 (1997) 4799–4808.
- [9] A.D. Brandon, R.J. Walker, J.W. Morgan, M.D. Norman, H.M. Prichard, Coupled ^{186}Os and ^{187}Os evidence for core-mantle interaction, *Science* 280 (1998) 1570–1573.
- [10] A.D. Brandon, M.D. Norman, R.J. Walker, J.W. Morgan, ^{186}Os – ^{187}Os systematics of Hawaiian picrites, *Earth Planet. Sci. Lett.* 174 (1999) 25–42.
- [11] J.M. Bird, A. Meibom, R. Frei, Th.F. Nägler, Osmium and lead isotopes of rare OsIrRu minerals: derivation from the core-mantle boundary region?, *Earth Planet. Sci. Lett.* 170 (1999) 83–92.
- [12] A. Meibom, R. Frei, Evidence for an ancient osmium isotopic reservoir in Earth, *Science* 296 (2002) 516–518.
- [13] L.M. Echeverria, Tertiary or Mesozoic komatiites from Gorgona Island, Field relations and geochemistry, *Contrib. Mineral. Petrol.* 73 (1980) 253–266.
- [14] M. Storey, J.J. Mahoney, L.W. Kroenke, A.D. Saunders, Are oceanic plateaus the site of komatiite formation?, *Geology* 19 (1991) 376–379.
- [15] N.T. Arndt, A.C. Kerr, J. Tarney, Dynamic melting in plume heads: The formation of Gorgona komatiites and basalts, *Earth Planet. Sci. Lett.* 146 (1996) 289–301.

- [16] A.C. Kerr, J. Tarney, G.F. Marriner, A. Nivia, A.D. Saunders, The Caribbean-Columbian Cretaceous igneous province: The internal anatomy of an oceanic plateau, in: J.J. Mahoney, M.F. Coffin (Eds.), *Large Igneous Provinces: Continental, Oceanic, and Planetary Volcanism*, Am. Geophys. Un. Geophys. Mon. 100, 1997, pp. 123–144.
- [17] S. Revillon, N.T. Arndt, C. Chauvel, E. Hallot, Geochemical study of ultramafic volcanic and plutonic rocks from Gorgona Island, Colombia: the plumbing system of an oceanic plateau, *J. Petrol.* 41 (2000) 1127–1153.
- [18] R.J. Walker, M. Storey, A.C. Kerr, J. Tarney, N.T. Arndt, Implications of ^{187}Os isotopic heterogeneities in a mantle plume: evidence from Gorgona Island and Curacao, *Geochim. Cosmochim. Acta* 63 (1999) 713–728.
- [19] R.J. Walker, L.M. Echeverria, S.B. Shirey, M.F. Horan, Re-Os isotopic constraints on the origin of volcanic rocks, Gorgona Island, Colombia: Os isotopic evidence for ancient heterogeneities in the mantle, *Contrib. Mineral. Petrol.* 107 (1991) 150–162.
- [20] S.B. Shirey, R.J. Walker, The Re-Os isotope system in cosmochemistry and high-temperature geochemistry, *Annu. Rev. Earth Planet. Sci.* 26 (1998) 423–500.
- [21] B.G. Aitken, L.M. Echeverria, Petrology and geochemistry of komatiites and tholeiites from Gorgona Island, Colombia, *Contrib. Mineral. Petrol.* 86 (1984) 94–105.
- [22] C.W. Sinton, R.A. Duncan, M. Storey, J. Lewis, J. Estrada, An oceanic flood basalt province at the core of the Caribbean plate, *Earth Planet. Sci. Lett.* 155 (1998) 221–235.
- [23] A.C. Kerr, G.F. Marriner, N.T. Arndt, J. Tarney, A. Nivia, A.D. Saunders, R.A. Duncan, The petrogenesis of Gorgona komatiites, picrites, and basalts: New field, petrographic, and geochemical constraints, *Lithos* 37 (1996) 246–260.
- [24] S.B. Shirey, R.J. Walker, Carius tube digestion for low-blank rhenium-osmium analysis, *Anal. Chem.* 34 (1995) 2136–2141.
- [25] J.W. Morgan, R.J. Walker, Isotopic determinations of rhenium and osmium in meteorites by using fusion, distillation, and ion-exchange separations, *Anal. Chim. Acta* 222 (1989) 291–300.
- [26] E.L. Hoffman, A.J. Naldrett, J.C. Van Loon, R.G.V. Hancock, A. Mason, The determination of all the platinum group elements and gold in rocks and ore by neutron activation analysis after preconcentration by a nickel sulfide fire-assay technique of large samples, *Anal. Chim. Acta* 102 (1978) 157–166.
- [27] A.S. Cohen, F.G. Waters, Separation of osmium from geological materials by solvent extraction for analysis by TIMS, *Anal. Chim. Acta* 332 (1996) 269–275.
- [28] J.L. Birck, M. Roy-Barman, F. Capmas, Re-Os isotopic measurements at the femtomole level in natural samples, *Geostand. Newslett.* 21 (1997) 19–27.
- [29] I.S. Puchtel, M. Humayun, Platinum group elements in Kostomuksha komatiites and basalts: Implications for oceanic crust recycling and core-mantle interaction, *Geochim. Cosmochim. Acta* 64 (2000) 4227–4242.
- [30] I.S. Puchtel, M. Humayun, Platinum group element fractionation in a komatiitic basalt lava lake, *Geochim. Cosmochim. Acta* 65 (2001) 2979–2993.
- [31] A.D. Brandon, J.E. Snow, R.J. Walker, J.W. Morgan, T.D. Mock, ^{190}Pt - ^{186}Os and ^{187}Re - ^{187}Os systematics of abyssal peridotites, *Earth Planet. Sci. Lett.* 177 (2000) 319–335.
- [32] G.D. Harper, The Josephine ophiolite, northwestern California, *Geol. Soc. Bull.* 95 (1984) 1009–1026.
- [33] T. Meisel, R.J. Walker, A.J. Irving, J.-P. Lorand, Osmium isotopic compositions of mantle xenoliths: A global perspective, *Geochim. Cosmochim. Acta* 65 (2001) 1311–1323.
- [34] E.H. Hauri, S.R. Hart, Re-Os isotope systematics of EMII and HIMU oceanic island basalts from the south Pacific Ocean, *Earth Planet. Sci. Lett.* 114 (1993) 353–371.
- [35] L.C. Reisberg, A. Zindler, F. Marcantonio, W.M. White, D. Wyman, B. Weaver, Os isotope systematics in ocean island basalts, *Earth Planet. Sci. Lett.* 120 (1993) 149–167.
- [36] A.W. Hofmann, Mantle geochemistry, the message from oceanic volcanism, *Nature* 385 (1997) 219–229.
- [37] G. Ravizza, J. Blusztajn, H.M. Pritchard, Re-Os systematics of platinum-group element distribution in metalliferous sediments from the Troodos ophiolite, *Earth Planet. Sci. Lett.* 188 (2001) 369–381.
- [38] W.J. Pegram, C.J. Allegre, Osmium isotopic compositions from oceanic basalts, *Earth Planet. Sci. Lett.* 111 (1992) 59–68.
- [39] M.D. Norman, M.O. Garcia, Primitive magmas and source characteristics of the Hawaiian plume petrology and geochemistry of shield picrites, *Earth Planet. Sci. Lett.* 168 (1999) 27–44.
- [40] B. Peucker-Ehrenbrink, G. Ravizza, The marine osmium isotope record, *Terra Nova* 12 (2000) 205–219.
- [41] D.K. McDaniel, R.J. Walker, Constraints on sources of osmium to the world's oceans: Combined $^{186}\text{Os}/^{188}\text{Os}$ and $^{187}\text{Os}/^{188}\text{Os}$ evidence, *EOS Trans. AGU* 82 (2001), Fall Meet. Suppl., pp. F1336–F1337.
- [42] J.C. Lassiter, E.H. Hauri, Osmium isotope variation in Hawaiian lavas: Evidence for recycled oceanic lithosphere in the Hawaiian plume, *Earth Planet. Sci. Lett.* 164 (1998) 483–496.
- [43] W.F. McDonough, S.-s. Sun, The composition of the Earth, *Chem. Geol.* 120 (1995) 223–253.
- [44] D. Walker, Core participation in mantle geochemistry, *Geochim. Cosmochim. Acta* 64 (2000) 2897–2911.
- [45] N.L. Chabot, A.J. Campbell, J.H. Jones, M. Humayun, C.B. Agee, An experimental test of Henry's Law in solid metal liquid–liquid systems with implications for iron meteorites, *Meteor. Planet. Sci.* (2002), in press.
- [46] R.J. Walker, H.M. Pritchard, A. Ishiwatari, M. Pimentel, The osmium isotopic composition of convecting upper mantle deduced from ophiolite chromites, *Geochim. Cosmochim. Acta* 66 (2002) 329–345.

- [47] J.E. Snow, L. Reisberg, Os isotopic systematics of altered abyssal peridotites, *Earth Planet. Sci. Lett.* 135 (1995) 411–421.
- [48] J.W. Morgan, M.F. Horan, R.J. Walker, J.N. Grossman, Rhenium-osmium concentration and isotope systematics in group IIAB iron meteorites, *Geochim. Cosmochim. Acta* 59 (1995) 2331–2344.
- [49] V.C. Bennett, T.M. Esat, M.D. Norman, Two mantle plume components in Hawaiian picrites inferred from correlated Os-Pb isotopes, *Nature* 381 (1996) 221–224.
- [50] R.J. Walker, J.W. Morgan, M.F. Horan, G.K. Czamanske, E.J. Krogstad, V.A. Fedorenko, V.E. Kunilov, Re-Os isotopic evidence for an enriched-mantle source for the Noril'sk-type, ore-bearing intrusions, Siberia, *Geochim. Cosmochim. Acta* 58 (1994) 4179–4197.
- [51] M.F. Horan, R.J. Walker, V.A. Fedorenko, G.K. Czamanske, Osmium and neodymium isotopic constraints on the temporal and spatial evolution of Siberian flood basalt sources, *Geochim. Cosmochim. Acta* 59 (1995) 5159–5168.
- [52] S.B. Shirey, Re-Os isotopic compositions of Midcontinent rift system picrites: implications for plume-lithosphere interaction and enriched mantle sources, *Can. J. Earth Sci.* 34 (1997) 489–503.
- [53] R.J. Walker, J.W. Morgan, E.J. Hanski, V. Smolkin, Re-Os systematics of Early Proterozoic ferropicrites, Pechenga Complex, NW Russia: evidence for ancient ^{187}Os enriched plumes, *Geochim. Cosmochim. Acta* 61 (1997) 3145–3160.
- [54] R.J. Walker, E. Nisbet, ^{187}Os isotopic constraints on Archean mantle dynamics, *Geochim. Cosmochim. Acta* 66 (2002) 3317–3325.
- [55] I.S. Puchtel, G.E. Brugmann, A.W. Hofmann, ^{187}Os -enriched domain in an Archean mantle plume, evidence from 2.8 Ga komatiites of the Kostomuksha greenstone belt, NW Baltic Shield, *Earth Planet. Sci. Lett.* 186 (2001) 513–526.
- [56] B.A. Buffett, H.E. Huppert, J.R. Lister, A.W. Woods, On the thermal evolution of the Earth's core, *J. Geophys. Res.* B 101 (1996) 7989–8006.
- [57] S. Labrosse, J.-P. Poirier, J.-L. LeMouel, On cooling of the Earth's core, *Phys. Earth Planet. Inter.* 99 (1997) 1–17.
- [58] J.R. Lister, B.A. Buffett, Stratification of the outer core at the core-mantle boundary, *Phys. Earth Planet. Inter.* 105 (1998) 5–19.
- [59] S. Labrosse, J.-P. Poirier, J.-L. LeMouel, The age of the inner core, *Earth Planet. Sci. Lett.* 190 (2001) 111–123.
- [60] C.K. Gessman, B.J. Wood, Potassium in the Earth's core?, *Earth Planet. Sci. Lett.* 200 (2002) 63–78.